

Gd₇I₁₂Zn: A Group 12 Atom in the Octahedral Gd₆ Cluster

Mar' yana Lukachuk,[†] Lorenz Kienle,[†] Chong Zheng,^{**‡} Hansjürgen Mattausch,[†] and Arndt Simon^{*†}

Max-Planck-Institut für Festkörperforschung, Heisenbergstrasse 1, D-70569 Stuttgart, Germany, and Department of Chemistry and Biochemistry, Northern Illinois University, DeKalb, Illinois 60115

Received January 6, 2008

The title compound was synthesized from Gd, GdI₃ and Zn under Ar atmosphere at 850 °C. It crystallizes in the space group $R\bar{3}$ (No. 148) with lattice constants $a = 15.686(1)$ Å and $c = 10.4882(8)$ Å. The structure features isolated Zn-centered Gd₆ octahedra with all edges and corners capped by I atoms. The disorder of the Gd atoms is rationalized via electron microscopic techniques. A computational analysis using the extended Hückel method has been carried out in order to understand the bonding of this compound. The structure of isotypic La₇I₁₂Co is also remarked ($a = 16.040(1)$ Å and $c = 10.905(2)$ Å).

Introduction

Reduced rare earth (R) metal halide chemistry has proven to be extremely rich, filled with novel crystal structures and unexpected physical properties. A central feature of the reduced rare earth halide compounds is their hosting capability. Many compounds in this category have been synthesized, with most of their structures consisting of octahedra or trigonal prisms of rare earth metal atoms centered by a variety of atoms.^{1–13} A quite common phase is R₇X₁₂Z, where X represents halogen atoms and Z represents main

group or transitional metal atoms. The electronic structure of these phases has been studied extensively.^{8–10,14–20} The electronic requirement is that there be no more than 8/6 electrons per cage R atom when Z is a transition metal, or one electron per cage R atom when Z is a main group element. However, this rule is not strictly followed.^{21,22} For example, Ni and Au can be included in the R₆X₁₂ cluster.^{9,22} In this contribution, we describe the synthesis and structure investigation by X-ray diffraction of two new compounds, Gd₇I₁₂Zn and La₇I₁₂Co. Gd₇I₁₂Zn is the first compound with a group 12 endohedral. Electron microscopy and bonding analyses of this compound have been carried out. The electron microscopy investigation focuses on one old and unresolved problem related to all structures of R₇X₁₂Z = R[R₆X₁₂Z] phases, namely, the unusual anisotropic atomic displacement parameters U_{11} and U_{33} of the isolated R atom.

Experimental Section

Synthesis. R (R = Gd, La) metal (sublimed, 99.99%; Alfa-Aesar, small pieces), RI₃, and T (T = Zn, Co; 99.99%; Aldrich) were used as starting materials. GdI₃ was synthesized from the reaction

* Authors to whom correspondence should be addressed. E-mail: A.Simon@fkf.mpg.de (A.S.); zheng@cz.chem.niu.edu (C.Z.).

[†] Max-Planck-Institut für Festkörperforschung.

[‡] Northern Illinois University.

- (1) Simon, A.; Mattausch, H.; Miller, G. J.; Bauhofer, W.; Kremer, R. K. Metal-Rich Halides. In *Handbook on the Physics and Chemistry of Rare Earths*; Elsevier Science Publishers: Amsterdam, 1991; Vol. 15, pp 191.
- (2) Mattausch, H.; Oeckler, O.; Simon, A. *Inorg. Chim. Acta* **1999**, 289, 174.
- (3) (a) Mattausch, H.; Simon, A. *Angew. Chem., Int. Ed.* **1998**, 37, 499. (b) Mattausch, H.; Simon, A. *Angew. Chem.* **1998**, 110, 498.
- (4) Warkentin, E.; Simon, A. *Rev. Chim. Miner.* **1983**, 20, 488.
- (5) Nagaki, D.; Simon, A.; Borrmann, H. *J. Less-Common Met.* **1989**, 156, 193.
- (6) Dorhout, P. K.; Payne, M. W.; Corbett, J. D. *Inorg. Chem.* **1991**, 30, 4960.
- (7) Llusar, R.; Corbett, J. D. *Inorg. Chem.* **1994**, 33, 849.
- (8) Hughbanks, T.; Rosenthal, G.; Corbett, J. D. *J. Am. Chem. Soc.* **1986**, 108, 8289.
- (9) Hughbanks, T.; Corbett, J. D. *Inorg. Chem.* **1988**, 27, 2022.
- (10) Hughbanks, T.; Corbett, J. D. *Inorg. Chem.* **1989**, 28, 631.
- (11) Meyer, G.; Wickleder, M. S. Simple and Complex Halides. In *Handbook on the Physics and Chemistry of Rare Earths*; Elsevier Science Publishers: Amsterdam, 2000; Vol. 28, Chapter 177, pp 53.
- (12) Corbett, J. D. *J. Chem. Soc., Dalton Trans.* **1996**, 575.
- (13) Jensen, E. A.; Corbett, J. D. *Inorg. Chem.* **2002**, 41, 6199.

- (14) Satpathy, S.; Andersen, O. K. *Inorg. Chem.* **1985**, 24, 2604.
- (15) Zheng, C.; Oeckler, O.; Mattausch, H.; Simon, A. *Z. Anorg. Allg. Chem.* **2001**, 627, 2151.
- (16) Miller, G. J.; Burdett, J. K.; Schwarz, C.; Simon, A. *Inorg. Chem.* **1986**, 25, 4437.
- (17) Burdett, J. K.; Miller, G. J. *J. Am. Chem. Soc.* **1987**, 109, 4092.
- (18) Xu, G.-X.; Ren, J. *Lanthanide Actinide Res.* **1987**, 2, 67.
- (19) Gao, S.; Xu, G.-X.; Li, L.-M. *Inorg. Chem.* **1992**, 31, 4829.
- (20) Sweet, L. E.; Roy, L. E.; Meng, F.; Hughbanks, T. *J. Am. Chem. Soc.* **2006**, 128, 10193.
- (21) Payne, M. W.; Corbett, J. D. *Inorg. Chem.* **1990**, 29, 2246.
- (22) Mattausch, H.; Zheng, C.; Kienle, L.; Simon, A. *Z. Anorg. Allg. Chem.* **2004**, 630, 2367.

of Gd₂O₃ (99.9%) with HI and NH₄I; LaI₃ was obtained from the reaction of La with I₂, and the products were purified by sublimation. Due to air and moisture sensitivity of the reactants and products, all handling was carried out under an Ar atmosphere either in a glovebox or through the standard Schlenk technique.

The stoichiometric mixtures (1075 mg of GdI₃, 236 mg of Gd, 33 mg of Zn (Gd₇I₁₂Zn); 1039 mg of LaI₃, 210 mg of La, 29 mg of Co(La₇I₁₂Co) of the starting materials were arc-sealed in Ta tubes under an Ar atmosphere. These were then sealed inside silica glass ampoules under a vacuum of *ca.* 10⁻² mbar. After 18 days at 850 °C for Gd₇I₁₂Zn and 21 days at 800 °C for La₇I₁₂Co, the ampoules were opened under an Ar atmosphere. Many black, irregularly shaped single crystals were observed in the products. The yield, estimated from powder X-ray diffraction and Guinier measurements, was larger than 90% for Gd₇I₁₂Zn and approximately 50% for La₇I₁₂Co. Energy dispersive X-ray (EDX) analyses, using a TESCAN scanning electron microscope equipped with an Oxford detector, showed the presence of the component elements in an approximate atomic ratio of 7.8:11.1:1.1 (R/X/Z, average of seven spectra) for Gd₇I₁₂Zn and 7.0:12.3:0.7 (average of four spectra).

Structure Determination by Single Crystal X-Ray Diffraction. The reaction products were ground to a fine powder under an Ar atmosphere and sealed in a glass capillary for phase identification on a STADI P powder diffractometer (Stoe, Darmstadt), using Ge monochromatized Mo K α 1 radiation ($\lambda = 0.7093$ Å). Single crystals were transferred to glass capillaries under Na-dried paraffin oil and sealed under an Ar atmosphere. They were first examined by the precession technique before being characterized on a STOE IPDS II or a Bruker CCD diffractometer. The structure was solved with direct methods and full matrix least-squares refinement on F^2 carried out using the SHELXTL package.²³

The two compounds crystallize in the trigonal space group $R\bar{3}$ (No. 148), and $Z = 3$. Refinement in the accentric space group $R3^{24}$ did not lead to an improvement. The crystallographic information including the fractional coordinates and selected bond lengths is listed in Tables 1–3.

Structure Determination by High-Resolution Transmission Electron Microscopy. The real structure of Gd₇I₁₂Zn was characterized by high-resolution transmission electron microscopy (HRTEM) and selected area electron diffraction (SAED). The transfer of the sample was carried out under dry Ar by applying Schlenk techniques.²⁵ A perforated carbon/copper net served as support of the crystallites. The studies were performed with a Philips CM30 ST microscope equipped with a LaB₆ cathode. At 300 kV, the point resolution is 0.19 nm. HRTEM images were calculated with the EMS program package²⁶ using the multislice formalism (parameters: Cs = 1.15 mm, $\Delta = 7$ nm, $\alpha = 1.2$ mrad).

Computational Study. The density of states (DOS) and the crystal orbital overlap population (COOP)²⁷ curves were computed using the tight-binding extended Hückel method (EH).^{28,29} A total of 256 k points in the irreducible wedge of the Brillouin zone were used in the EH computation of the DOS and COOP curves based on the EH parameters listed in Table 4.

Table 1. Crystal Data and Structure Refinement for Gd₇I₁₂Zn and La₇I₁₂Co

empirical formula	Gd ₇ I ₁₂ Zn	La ₇ I ₁₂ Co
formula weight	2688.92	2554.10
space group	$R\bar{3}$ (No. 148)	$R\bar{3}$ (No. 148)
unit cell dimensions, a (Å)	15.686(1)	16.040(1)
c (Å)	10.4882(8)	10.905(2)
V (Å ³)	2234.9(3)	2429.7(4)
Z	3	3
calcd density (g/cm ³)	5.994	5.237
cryst size (mm ³)	0.18 × 0.13 × 0.08	0.18 × 0.12 × 0.03
max. and min. transmission	0.2895/0.0526	0.4194/0.0166
abs. coeff. (mm ⁻¹)	28.554	20.937
F (000)	3342	3186
θ range (deg)	2.45 to 29.99	2.37 to 25.00
range in hkl	$-18 \leq h \leq 22$ $-22 \leq k \leq 22$ $-14 \leq l \leq 13$	$-19 \leq h \leq 19$ $-19 \leq k \leq 18$ $-12 \leq l \leq 12$
total no. reflns	7709	6043
independent reflns [R_{int}]	1446 [0.0408]	949 [0.0409]
data/parameters	1446/35	949/35
goodness-of-fit on F^2	1.202	1.334
final R indices [$I > 2\sigma(I)$], R1	0.0265	0.0295
wR2	0.0459	0.0567
R indices (all data), ^a R1	0.0344	0.0342
wR2	0.0475	0.0577
largest diff. peak and hole (e/Å ³)	1.279/−1.071	0.894/−0.853

$$^a R1 = \sum |F_o| - |F_c| / \sum |F_o|. \text{ wR2} = \{ \sum [w(F_o^2 - F_c^2)^2] / \sum [w(F_o^2)^2] \}^{1/2}.$$

Table 2. Atomic Coordinates and Equivalent Isotropic Displacement Parameters (Å²) for Gd₇I₁₂Zn and La₇I₁₂Co^a

atom	Wyck.	occ.	x	y	z	U_{eq}
Gd ₇ I ₁₂ Zn						
Gd1	18f	1.00	0.1695(1)	0.5494(1)	0.0125(1)	0.015(1)
Gd2	6c	0.494(2)	0	0	0.0265(1)	0.020(1)
I1	18f	1.00	0.4125(1)	0.4323(1)	0.1644(1)	0.023(1)
I2	18f	1.00	0.4791(1)	0.1989(1)	0.1749(1)	0.023(1)
Zn	3b	1.00	0	0	1/2	0.013(1)
La ₇ I ₁₂ Co						
La(1)	18f	1.00	0.1731(1)	0.5508(1)	0.0163(1)	0.020(1)
La(2)	6c	0.496(3)	0	0	0.0246(2)	0.024(1)
I(1)	18f	1.00	0.4121(1)	0.4318(1)	0.1640(1)	0.034(1)
I(2)	18f	1.00	0.4776(1)	0.1971(1)	0.1762(1)	0.029(1)
Co	3b	1.00	0	0	1/2	0.017(1)

^a U_{eq} is defined as one third of the trace of the orthogonalized U_{ij} tensor.

Table 3. Selected Bond Lengths [Å] for R₇I₁₂M (R = Gd, La; T = Zn, Co)

bond	Gd ₇ I ₁₂ Zn	La ₇ I ₁₂ Co
R1–R1 (×2)	3.9657(5)	3.9817(7)
R1–R1 (×2)	3.9730(6)	4.0042(8)
R1–R2 (×1)	4.0587(7)	4.225(2)
R1–I1 (×1)	3.1333(4)	3.2340(6)
R1–I1 (×1)	3.1600(4)	3.2383(6)
R1–I1 (×1)	3.2393(4)	3.3909(6)
R1–I2 (×1)	3.1599(4)	3.2840(6)
R1–I2 (×1)	3.1635(4)	3.2912(6)
R2–I2 (×3)	2.9681(5)	3.071(1)
R2–I2 (×3)	3.2647(5)	3.357(1)
R1–T (×1)	2.8068(3)	2.8234(5)

Results and Discussion

Endohedral transition metal atoms, for example, Co, have been repeatedly identified in octahedral cages of rare earth

(23) Sheldrick, G. M. *SHELXTL*, version 6; Bruker Analytical X-ray Systems: Madison, WI, 2000.

(24) Dudis, D. S.; Corbett, J. D.; Hwu, S.-J. *Inorg. Chem.* **1986**, *25*, 3434.

(25) Jeitschko, P.; Simon, A.; Ramlau, R.; Mattausch, H. *Eur. Microscopy Microanal.* **1997**, *46*, 21.

(26) Stadelmann, P. A. *Ultramicroscopy* **1987**, *21*, 131.

(27) Wijeyesekera, S. D.; Hoffmann, R. *Organometallics* **1984**, *3*, 949.

(28) Whangbo, M. H.; Hoffmann, R.; Woodward, R. B. *Proc. R. Soc. London* **1979**, *A366*, 23.

(29) Hoffmann, R. *J. Chem. Phys.* **1963**, *39*, 1397.

(30) Previously, we used the term “interstitial”. However, this leaves an ambiguity as the additional atom can occur inside the cluster or in voids between the clusters. The term “endohedral” is therefore used for an atom inside the cluster.

Table 4. Extended Hückel Parameters

	orbital	H_{ii} (eV)	ζ_1^a	ζ_2	c_1^a	c_2
Gd	6s	-7.67	2.14			
	6p	-5.01	2.08			
	5d	-8.21	3.78	1.381	0.7765	0.4587
I	5s	-18.0	2.679			
	5p	-12.7	2.322			
Zn	4s	-9.391	2.01			
	4p	-5.163	1.70			
	3d	-17.302	6.15	2.600	0.5900	0.5700

^a Exponents and coefficients in a double- ζ expansion of the d orbital.

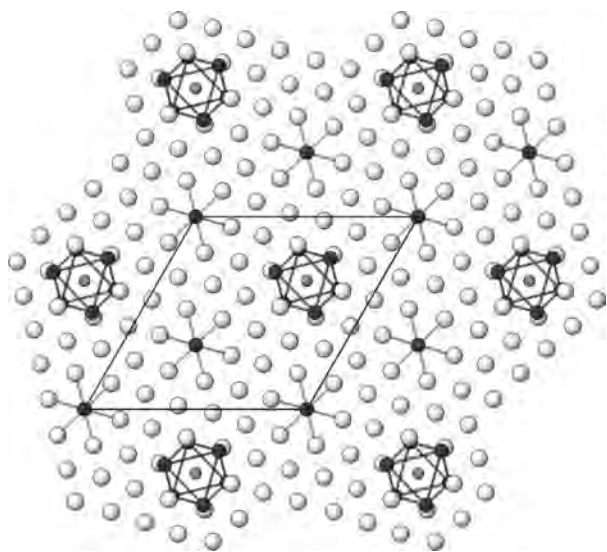


Figure 1. Section $-0.19 \leq z \leq 0.57$ of the $\text{Gd}_7\text{I}_{12}\text{Zn}$ structure along [001]. The Zn atom is at the center of the Gd_6 octahedron.

metal clusters.³⁰ However, $\text{Gd}_7\text{I}_{12}\text{Zn}$ is the first representative of a cluster with an endohedral Zn atom. This fact is somewhat surprising as there exists a rich chemistry of R/Zn intermetallics,³¹ indicating the mutual affinity of these elements, as also clearly evident from the Miedema rule.³²

Crystal Structure. $\text{Gd}_7\text{I}_{12}\text{Zn}$ and $\text{La}_7\text{I}_{12}\text{Co}$ are isostructural to $\text{Sc}_7\text{Cl}_{12}\text{C}$.²⁴ For the Gd compound, Gd1 (at Wyckoff site 18f in Table 2) forms octahedra with a Gd–Gd distance of 3.97 Å. The 12 edges of the metal octahedron are capped by I atoms with Gd–I distances (Gd1–I1 in Table 3) of around 3.13–3.16 Å. The six corners of the octahedron are also capped by I atoms from adjacent Gd_6I_{12} clusters. The terminal Gd–I distance (also Gd1–I1 in Table 3) is slightly larger at 3.24 Å. Figure 1 shows the structure viewed down the c axis. In the figure, the I atoms form a close-packed arrangement but with one atom replaced by the endohedral atom Zn (gray spheres). The Gd_6 octahedron is oriented in such a way that two of its opposite triangular faces are perpendicular to the c axis. Gd2 (at Wyckoff site 6c) are located above and below these two triangular faces at a Gd1–Gd2 distance of 4.06 Å. The I atoms capping six edges in the waist of such an oriented octahedron are also bonded

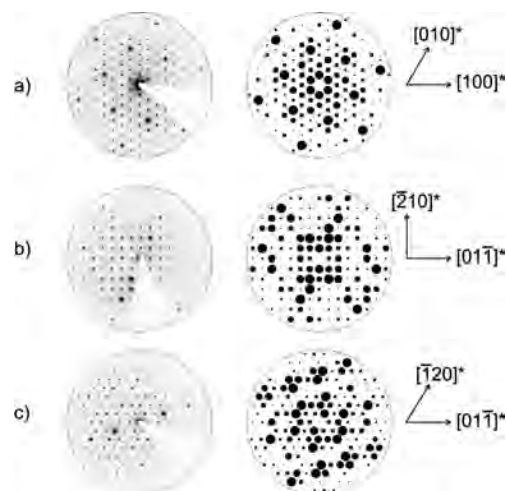


Figure 2. SAED patterns of $\text{Gd}_7\text{I}_{12}\text{Zn}$ and simulations for zone axes orientations (a) [001], (b) [122], and (c) [211].

to the corners of adjacent Gd_6 octahedra. Using the notation of Schäfer and Schnering,³³ we can write the formula for the octahedral cluster as $(\text{Gd}_2)(\text{Gd}_1)_6\text{I}_6\text{I}^{i-a}_{6/2}\text{I}^{a-i}_{6/2}\text{Zn}$. Gd2 atoms are coordinated octahedrally to I atoms (black noncage spheres in Figure 1). Therefore, one would expect a rather spherical shape of the atomic anisotropic displacement ellipsoid. However, the structure refinement with Gd2 atoms in the 3a Wyckoff position resulted in high anisotropic displacement parameters with a ratio $U_{33}/U_{11} \approx 8$. This unusual ratio has been observed for all reported structures of $\text{R}_7\text{X}_{12}\text{Z}$ phases. The splitting of this position by setting a free z parameter led to significant improvement. Therefore, Gd2 atoms were refined in the 6c Wyckoff position with an occupancy of 49.4(2)%. The same treatment was applied to the La compounds.

Electron Microscopy Investigation of Disorder. As is well-known, the disorder in average structures is frequently caused by the superposition of domains with ordered structure. For $\text{Gd}_7\text{I}_{12}\text{Zn}$, a large number of crystallites was investigated. In the following, a series of representative results is reproduced. It should be mentioned that, even with an isotopic phase where Zn is replaced by Ga, similar results were obtained.³⁴ No indications for ordering, such as superstructure reflections or diffuse scattering, were found in all $[uvw]$ SAED patterns, with $w \neq 0$; compare the examples in Figure 2. These patterns are consistent with the metrics of the average structure, and their intensity is convincingly reproduced by kinematical simulations when transmitting thin areas.

The characteristic disorder, that is, the split positions of Gd2 along [001], is revealed upon further examinations of zone axes $[uw0]$. Thicker areas exhibit no signs of ordering. Particularly, bright-field images demonstrate the absence of microdomains with ordered structure. HRTEM micrographs are consistent with the average structure, see Figure 3c for zone axis [210] and Scherzer focus. The periodic pattern of white spots, representing the cavities of the structure, is fully

(31) Villars, P.; Calvert, L. D. *Pearson's Handbook of Crystallographic Data for Intermetallic Phases*, 2nd ed.; ASM International: Materials Park, OH, 1991; Vol. 4.

(32) Miedema, A. R.; Boom, R.; de Boer, F. R. Simple Rules for Alloying. In *Crystal Structure and Chemical Bonding in Inorganic Chemistry*; Rooymans, C. J. M., Rabenau, A., Eds.; North-Holland: Amsterdam, 1975.

(33) Schäfer, H.; Schnering, H. G. *Angew. Chem., Int. Ed.* **1964**, 76, 833.

(34) Kienle, L.; Lukachuk, M.; Duppel, V.; Mattausch, H.; Simon, A. Z. *Anorg. Allg. Chem.* **2007**, 633, 1708.

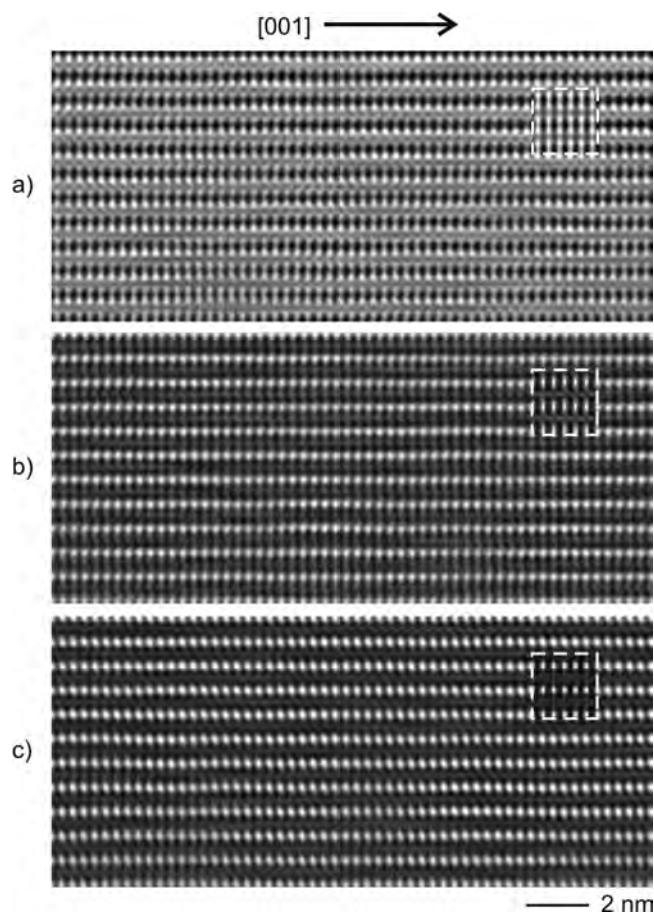


Figure 3. HRTEM micrographs with inserted simulation [zone axis [210], $t = 5.4$ nm, (a) $\Delta f = +25$ nm, (b) $\Delta f = -25$ nm, (c) $\Delta f = -65$ nm].

consistent with the inserted simulated micrograph, which is based on the average structure. No significant variations of the contrast along [001] occur, even for the defocus values in Figure 3a and b. Hence, ordering of Gd2 is not significant.

All observations described so far initiated the search for low-symmetry structure models with a marginal significance of the ordering. First, we checked for an absence of the inversion center and created a structure model in the maximum $i2$ subgroup of the average structure according to Dudis et al.²⁴ The Wyckoff site $6a$ ($R\bar{3}$) splits into symmetry-independent positions $3a$ ($R3$). The split position in the average structure could then be rationalized by assuming inversion domains, and simulations based on noncentrosymmetric models correlate with the low significance of the ordering.

However, examinations on thin areas of zone axes $[uv0]$ reveal significant deviations from the average structure and indicate an alternative. The ordering is not the result of decomposition in surface layers as confirmed by EDX. In the SAED patterns, reflections on positions $hkl/2$ are clearly visible, as demonstrated for [210] in Figure 4a, left. The intensity of these superstructure reflections varied in neighboring areas of the same crystal and was strongly reduced when transmitting thicker areas. In the latter case, only a few streaks on $hkl/2$ can be seen in the diffraction patterns, see the arrows in Figure 4a, right. For the interpretation of HRTEM micrographs, a structure model with doubled unit

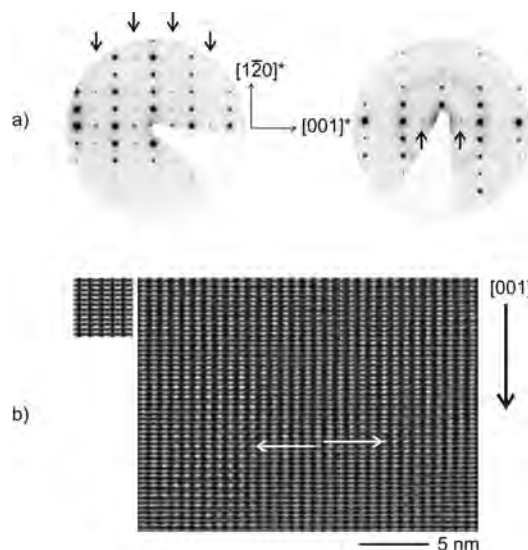


Figure 4. (a) SAED patterns for [210] with superstructure reflections on positions $hkl/2$ (left, thin area; right, thick area). (b) HRTEM micrograph with simulation ($t = 2.7$ nm, $\Delta f = +35$ nm) indicating the ordering and the shift of neighboring nanodomains.

cell volume ($R\bar{3}$, $c' = 2c$) was created which enables restricting Gd2 to alternating fully and non-occupied sites $6c$ along [001]. With respect to the average structure, a symmetry reduction ($i2$) occurs which clearly contrasts with the t -type transition mentioned above. Only the $i2$ model of ordering is consistent with the observations. Simulated SAED patterns reproduce the superstructure reflections, and in accordance with simulated micrographs, the ordering can only be visualized when selecting overfocus, see the consecutive brighter and darker spots along [001] in Figure 4b. Underfocus conditions eliminate the significance of the ordering. The image of Figure 4b also displays the characteristic domain structure associated with the i -type group-subgroup relation of averaged and real structure.³⁵ Neighboring domains with clear ordering along [001] are shifted by one unit length c , compare the arrows in Figure 4b. The coexistence of such nanoscale antiphase domains (nAPD) explains the split position of Gd2 in the average structure. A shift of c causes superposition of all atoms, except for Gd2, which transforms into the closely neighboring off-center positions within the I_6 octahedra. Therefore, the average structure is an artifact based on the superposition of nAPD's with ordering of Gd2 along [001]. Neighboring nAPD's are separated by areas of overlap which do not show any ordering due to the superposition along the zone axes. Strong space averaging which is particularly expected for the thick areas inhibits the detection of ordering; hence, very low intensity of the superstructure reflections is observed. A careful examination of the corresponding X-ray patterns does not reveal any superstructure reflections or diffuse scattering, obviously due to enhanced space averaging.

Electronic Structure. The electronic structure of an isolated rare earth metal octahedral cluster is well-known.^{1,14–20,22} In the case of a transition metal endohedral, a triply degenerate t_{1u} level and an a_{1g} orbital contributing to

(35) Bärmighausen, H. *MATCH* 1980, 9, 139.

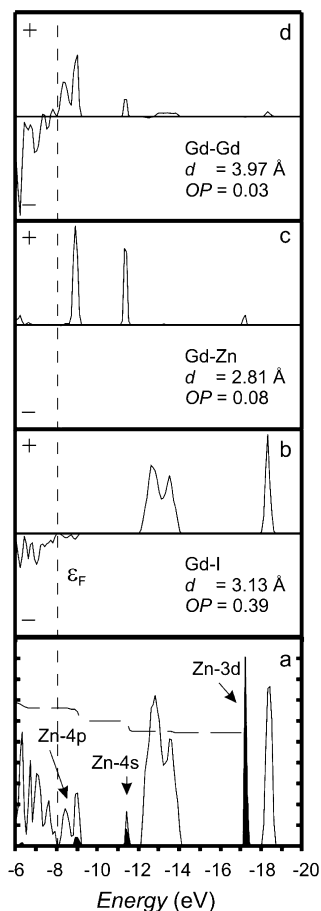


Figure 5. EH DOS and COOP plots for the idealized $\text{Gd}_7\text{I}_{12}\text{Zn}$ structure. (a) DOS: The solid line is the total DOS, the dashed line is the integrated Zn DOS, and the shaded area is the contribution from Zn. The vertical dashed line indicates the Fermi level. (b–d) EH COOP curves for representative bonds in $\text{Gd}_7\text{I}_{12}\text{Zn}$. The + region is bonding area and the – region is the antibonding area. The bond type, distance (d), and integrated overlap population (OP) to the Fermi level are indicated in the panel.

metal–metal bonding can be filled, and in some cases, still another a_{2u} orbital can be occupied. Thus, a total of eight electrons can be accommodated per octahedron. $\text{La}_7\text{I}_{12}\text{Co}$ obeys this rule. However, this rule is not strictly followed.^{21,22} For $\text{Gd}_7\text{I}_{12}\text{Zn}$, the EH DOS and COOP curves were computed for an idealized $\text{Gd}_7\text{I}_{12}\text{Zn}$ structure without the split positions. Figure 5, parts b–d are the COOP curves of relevant atomic contacts in the structure. All of them contribute to bonding below the Fermi level.

Figure 5a shows the projected Zn DOS (shaded area) together with the total DOS. The lowest peak is the I 5s orbital, then come the Zn 3d, I 5p, Zn 4s, Zn 4p, and Gd 5d states in order of increasing energy. The Zn 3d orbital lies very low in energy, as expected, and in effect, Zn acts as an

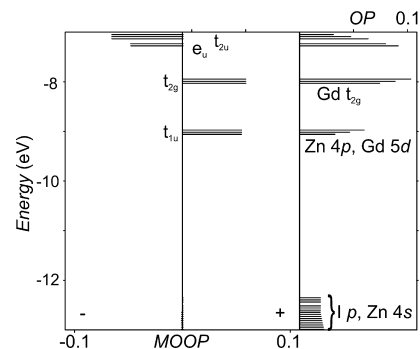


Figure 6. MOOP plot for an isolated $\text{Gd}_6\text{I}_{18}\text{Zn}$ cluster.

s–p metal. The most important feature here is the Gd–Gd COOP curve showing bonding below and near the Fermi level. This feature can be understood from the EH molecular orbital overlap populations (MOOP)³⁶ calculated for an isolated $\text{Gd}_6\text{I}_{18}\text{Zn}$ cluster taken out from the idealized $\text{Gd}_7\text{I}_{12}\text{Zn}$ structure. The MOOP in Figure 6 reveals that above the I 5p and Zn 4s orbitals there are orbitals of t_{1u} symmetry originating from Zn 4p and Gd 5d states, and three Gd 5d orbitals of t_{2g} symmetry with no admixture of Zn states. All of them can be occupied without contributing to antibonding states of the Gd_6 cage.

The electron partitioning in $\text{Gd}_7\text{I}_{12}\text{Zn}$ can be formalized within the ionic limit of the Zintl–Klemm concept as $(\text{Gd}^{3+})_7(\text{I}^-)_{12}\text{Zn}^{6-} \cdot 3e^-$ with three skeleton electrons shared among the six cage Gd atoms, and the rule of a maximum of one electron per cage Gd atom is followed as in the case of a main group endohedral. This assignment falls in line with a formal description of other endohedrals, H, O, N, C, and B, the “charges” decreasing stepwise from –1 to –5. However, as the integrated DOS in Figure 5a indicates, the Zn 4p bands are only partly filled and the EH charge of zinc is actually Zn^0 inside the $[\text{Gd}_6\text{Zn}]^{9+}$ cluster.

Acknowledgment. We thank Viola Duppel and Claudia Kamella for the HRTEM and EDX measurements, respectively, Eva Brücher for the magnetic susceptibility measurements, and Constantin Hoch for the X-ray data collection. C.Z. acknowledges the support by the Max-Planck-Gesellschaft, which made his visit at MPI possible.

Supporting Information Available: Listing of X-ray crystallographic details in CIF format. This material is available free of charge via the Internet at <http://pubs.acs.org>.

IC800024N

(36) Mealli, C.; Proserpio, D. M. *J. Chem. Educ.* **1990**, *67*, 399.